Analysis of Immunity Failures and Optimization Measures in Automotive Sensors

Jan Benz, Andreas Klaedtke, Jan Hansen
Robert Bosch GmbH
Reutlingen, Germany
jan.benz2@de.bosch.com

Stephan Frei
TU Dortmund University
Dortmund, Germany
stephan.frei@tu-dortmund.de

***Abstract*—Automotive sensors need to fulfill severe electromagnetic compatibility (EMC) requirements. The space available for EMC solutions based on discrete filter elements is limited. Furthermore, direct voltage or current measurements for analysis purposes are difficult. Innovative simulation methods are therefore needed to further understand and develop non-conventional EMC solutions. In this paper an analysis method to extract the dominant coupling path within sensors and to generate minimized electrical equivalent circuits (EEC) using network based sensitivity analysis is presented. In addition, a computational method that indicates the hotspots causing the EMC immunity failures with high resolution is introduced. Consequently, potential geometric and layout optimizations are derived easily. Failures due to small asymmetries are finally analyzed and optimized using an automotive pressure sensor.**

***Index Terms*—Bulk Current Injection (BCI), Sensitivity Analysis, Sensor Immunity, PHREEC**

I. Introduction

Vehicle electrification and autonomous driving increase the need for automotive sensors. Even today's cars contain several dozens of sensors controlling comfort functions (air conditioning etc.), drivetrain functions (exhaust after treatment, battery thermal management, etc.) as well as safety critical functions like the antilock braking system, the electronic stability control and the airbag system. In principle, many automotive sensors consist of two main components: A microelectromechanical system (MEMS) and an application-specific integrated circuit (ASIC). The MEMS converts a mechanical quantity (pressure, acceleration, yaw rate, etc.) into an electrical quantity. The ASIC processes and converts the often small MEMS currents and voltages by an analog-to-digital converter (ADC) and communicates with the electronic control unit (ECU). The connection between MEMS and ASIC, often called front-end, represents the most sensitive part of sensors [1], [2]. Fig. 1 illustrates the general setup of many automotive sensors. It can be seen, that only the ASIC is protected by filter elements. Additional filter elements in the sensitive front-end are difficult to integrate due to the limited space available.

To ensure proper operation in a severe electromagnetic environment, automotive sensors have to endure harsh electromagnetic compatibility (EMC) tests. In the majority of immunity tests, a high common mode (CM) current is impressed into the sensor. Due to asymmetrical couplings, the common mode can

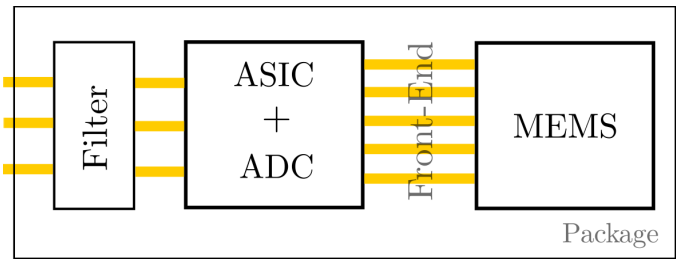

Fig. 1: Simplified schematic setup of typical automotive sensors

be converted into a differential mode (DM), which can disturb the desired signals. The most critical part of the signals to be disturbed is the front-end, where some additional μV can cause the sensor to fail [2].

A root cause analysis of these small front-end voltages with measurements is very difficult in most cases due to the small-sized sensors. Furthermore, additional measurement equipment alters the test environment due to an impedance change within the sensor, e.g. a directly connected probe changes the capacitive coupling in a floating DUT dramatically. The mere simulation of the small front-end couplings, presented in [3], will be used as starting point to further investigate the front-end coupling. The analog front-end voltage is therefore transformed into the digital signals of the sensor - also known as least significant bits (LSB).

Due to the high quantity of produced sensors, it is advantageous to optimize the geometry or layout of the sensor, instead of using additional filter components.

In this paper, a novel method to easily tackle root cause analyses of sensor immunity failures and a subsequent geometry optimization is presented. Three steps are carried out. First, a physical reduced equivalent electrical circuit (PHREEC: [4], [5], [6], [7]) is constructed. In a second step, a root cause analysis of the coupling effect is performed with the help of a network based sensitivity analysis. The resulting minimized circuit simulations show good correlation to common 3D-simulations. Third, a 3D sensitivity analysis based on the work in [8], [9] and [10] is performed using automotive pressure sensors. The 3D sensitivity analysis highlights potential layout/geometry optimizations by combining

978-1-7281-0594-9/19/$31.00 © 2019 IEEE

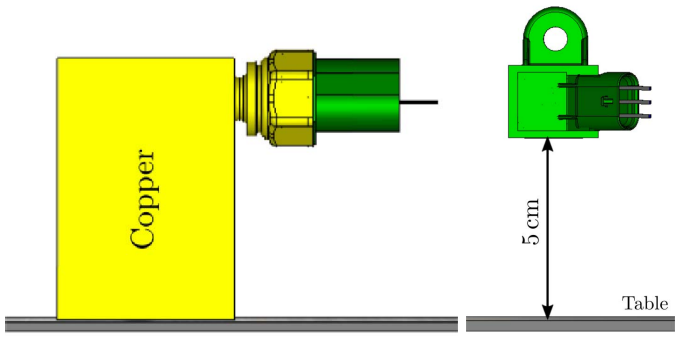

(a) locally grounded setup (b) floating setup

Fig. 2: Different sensor BCI setups

geometric sensitivities with network sensitivities. Finally, a simulation-based optimization of the front-end coupling, using the above-mentioned methods, is carried out on a pressure sensor. Measurements validate the simulations and show an improvement of the sensor immunity by a factor of four.

II. Theory and Workflow

This section motivates and presents the novel workflow performed in this paper. Fundamentals of the BCI simulation environment, the PHREEC method and the 3D sensitivity analysis procedure are given. The goal is to identify, investigate and optimize the dominant parasitics for a pre-defined Quantity of Interest (QoI) [8]. A Quantity of Interest is any 1D quantity of the network simulation, be it a voltage, a current or even an impedance. Here, the front-end voltage at the ASIC's ADC, which is the most sensitive and critical part of a sensor, is used as QoI [3].

A. BCI Simulation

A high power level in combination with a highly resonant setup (mismatched harness) in the Bulk Current Injection (BCI) test leads to one of the toughest immunity test requirements for sensor. Especially the closed-loop method injects a high common mode and causes the majority of sensor EMC problems. Therefore, all simulations and measurements are based on a closed-loop BCI test from 0.1-400 MHz with a 300 mA current limit.

The setup consists of injection and monitoring clamp, harness, ECU emulation (loadbox), line impedance stabilization network (LISN) and the DUT (here: automotive pressure sensor). Depending on the termination in the final application, sensors can be differentiated between floating sensors (in the test setup the sensor floats 5 cm above the table; no direct ground connection) and locally grounded sensors (sensor fixed in copper block; inductive connection to ground). This is due to the fact, that some sensors are later screwed into the car's engine. The two setups are shown in Fig. 2. For the BCI simulation the methods shown in [11], [12] and [13] are used. Furthermore, the LSB deviation of the sensor signals are simulated using [3]. LSBs describe the smallest unit a sensor can measure. E.g. if the sensor can dissolve 0.1 kPa and a deviation of 100 LSB is measured, the sensor measures an error due to EMI equivalent to 10 kPa.

Fig. 3 shows the simulated and measured maximum pressure signal LSB deviation of a floating sensor during closed-loop BCI with a 300 mA current limit. A good correlation between the measured and simulated LSB can be seen. The high simulation accuracy enables a precise root cause analysis and the optimization of small couplings.

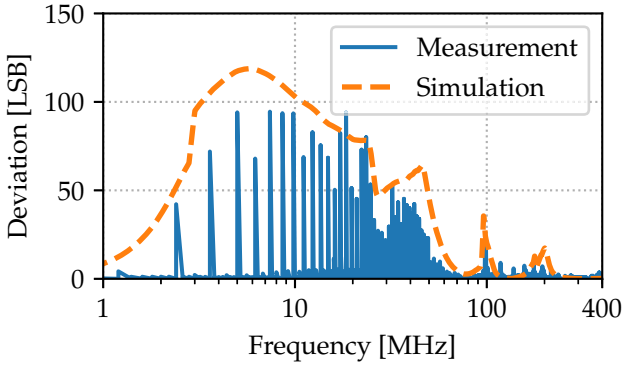

Fig. 3: Measured and simulated LSB deviation in a 300 mA closed-loop BCI test

B. Physically Reduced Equivalent Electrical Circuits (PHREEC)

The PHREEC method presented in [4] - [7] is used to generate the equivalent electrical circuits (EECs). It extracts EECs which are networks of parasitic partial inductances L, capacitances C and ohmic resistances R between user defined terminals from a 3D model. Serial capacitances are extracted within the electrostatic approximation to Maxwells equations [5]. Partial self and mutual inductances, and equivalent parallel capacitances (EPCs) are extracted within the Darwin approximation to Maxwells equations using the Lorenz gauge [5]. Retardation effects are not considered but, because of the small DUT size l of less than the wavelength λ, the solutions hold up to frequencies above 1 GHz. The partial differential equation systems describing the electromagnetic fields are discretized and solved using the finite element method (FEM).

C. Sensitivity Analysis

The PHREEC method generates R, C, L matrices consisting of a large number of components (depending on the number of terminals), rendering a manual root cause analysis impossible. For an average sensor around 40 terminals are needed resulting in over 1500 parasitics. A reduction to an essential, bare minimum number of parasitics that is relevant to the investigated effect is required to allow for an efficient manual analysis. Hence, a sensitivity analysis on network level of the BCI frequency range (0.1-400 MHz) is set up to extract the most sensitive parasitics with respect to the QoI. The functional

components (discrete filter elements, internal MEMS and ASIC parasitics, etc.) are added to the extracted parasitics in a system simulation. The BCI excitation is simplified by a common mode current source between the connector and table.

In a circuit simulator the sensitivities are calculated and normalized (each matrix element separately) with respect to the parasitic parameters and the QoI. The parasitics with a negligible magnitude of the sensitivity are dropped. The remaining parasitics together with the functional components are included in the BCI simulation presented in Section II A. Finally, the LSB deviation of the sensor signal is calculated in a closed-loop BCI test with a significantly reduced, but accurate electrical equivalent circuit (EEC) of the sensor. Due to the physical relation between EEC and 3D model, geometry analysis is possible.

D. 3D Sensitivity Analysis

In addition to a root cause analysis and the synthesis of a minimized EEC, this section presents a 3D optimization method based on the work shown in [8], [9] and [10].

The use of the network sensitivities calculated in the previous section in combination with a geometric sensitivity analysis, indicates the hotspot causing the EMC immunity failures. This 3D sensitivity analysis points to areas in the model geometry, which show potential for optimizations. To achieve this, the unnormalized network sensitivities

$$\mathbf{S}_{net}(\omega) = \frac{\partial Q(\mathbf{z})}{\partial \mathbf{z}} \tag{1}$$

and the geometric sensitivities

$$\mathbf{S}_{geo}(\omega) = \frac{d\mathbf{z}}{dp_i} \tag{2}$$

are combined. Here, $\mathbf{z}$ are the network impedances (matrix-variate and stacked into a vector), Q is the QoI and p_i are the geometric model parameters, e.g. the vertex positions in the FEM mesh. The application of the chain rule combines the network and geometric sensitivities of the QoI to model parameter changes,

$$\frac{dQ(\omega)}{dp_i} = \underbrace{\left(\frac{\partial Q(\mathbf{z})}{\partial \mathbf{z}}\right)^T}_{\mathbf{S}_{\text{net}}(\omega)} \cdot \underbrace{\frac{d\mathbf{z}}{dp_i}}_{\mathbf{S}_{\text{geo}}(\omega)} . \tag{3}$$

A sensitive regions means, that a vertical translation of the surface element will significantly influence the QoI. The higher the color saturation, the bigger the effect on the QoI.

III. System Analysis

Two automotive sensors are investigated. The dominant front-end coupling paths are extracted by creating minimized EECs. As a result of the 3D sensitivity analysis, potential optimizations are highlighted and interpreted.

A. Floating Sensor

1) EEC: Fig. 4 shows the circuit (using PHREEC and a subsequent sensitivity analysis) of the floating sensor presented in Fig. 2b. The network level sensitivity analysis proves that mainly capacitances are sensitive. Besides the parasitic capacitances $C_{R1} - C_{R4}$ of the Wheatstone bridge and the parasitic capacitances C_{ESD} of the electrostatic discharge (ESD) protection diodes inside the ASIC, only the parasitic capacitances C_1 and C_2 contribute to the front-end coupling. In particular, the sensitivities of C_1 and C_2 are at least an order of magnitude larger than all other elements.

A good correlation between a 3D simulation and the minimized circuit simulation (Fig. 4) is displayed in Fig. 5. With the exception of the resonance at 30 MHz, the difference between the time consuming 3D simulation and the minimized EEC is less than 10 LSB.

Because the ADC evaluates a differential voltage, while the BCI test excites a common mode voltage between sensor and table, the coupling mainly arises due to an asymmetrical layout coupling between front-end and common ground (table) (here: C_1 and C_2). The difference in those two capacitances adds up to a value smaller 1 fF, causing the sensor to fail the BCI test. As a design rule, similar capacitances C_1 and C_2 of the front-end structure to the table are needed to enforce a symmetrical capacitive coupling and therefore less CM-to-DM conversion.

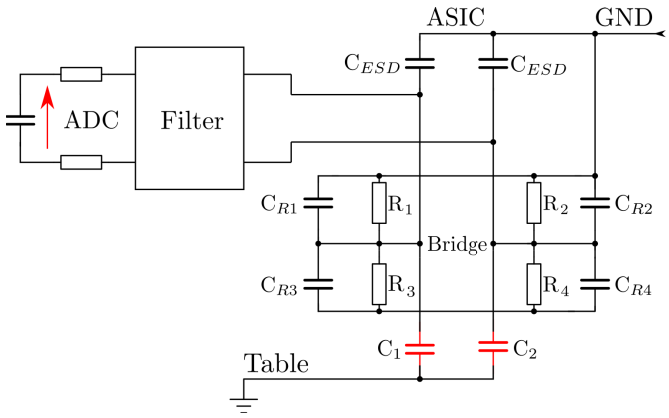

Fig. 4: EEC of the front-end coupling of a floating pressure sensor using PHREEC and a subsequent network sensitivity analysis

2) 3D Sensitivity Analysis: To extract potential geometric or layout optimizations a 3D sensitivity analysis of the investigated asymmetric, capacitive coupling is performed. Fig. 6 shows the 3D sensitivities of the critical front-end section of the floating pressure sensor in Fig. 2b. The figure shows the layout between the ASIC and the vias on the top layer of the PCB. In addition, Fig. 7 shows the layout between the MEMS and the vias on the bottom layer of the PCB. The red colored trace T_4 is represented in the EEC with the capacitance C_1 and the blue colored trace T_3 is represented with the capacitance C_2.

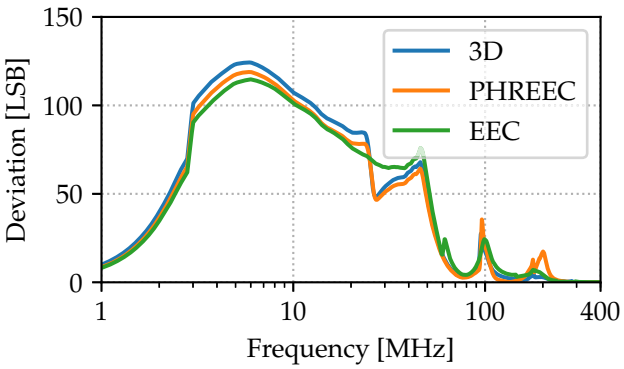

Fig. 5: Simulation of the LSB deviation using the 3D model, the physical reduced equivalent electrical circuit (PHREEC) model and the minimized EEC model in Fig. 4 in a 300 mA closed-loop BCI test

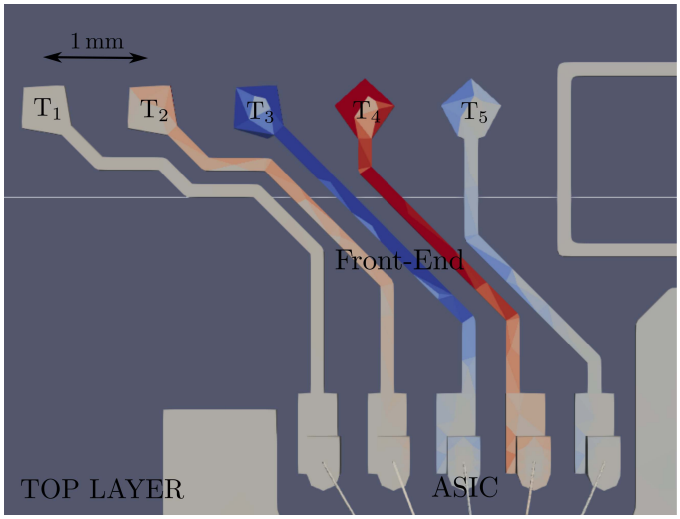

Fig. 6: 3D sensitivity analysis of the front-end coupling of the top layer section

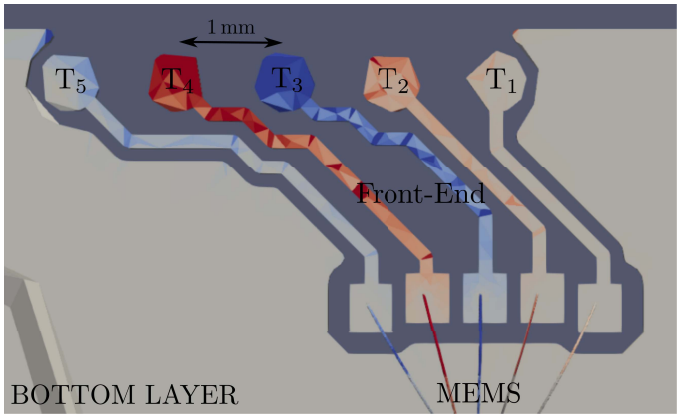

Fig. 7: 3D sensitivity analysis of the front-end coupling of the bottom layer section

3) Interpretation: The asymmetrical capacitive coupling (C_1>C_2), already extracted in the network sensitivity analysis, can be seen again. Furthermore, the most sensitive geometry parts are highlighted, which can be used to understand potential geometric optimizations. The following interpretations can be drawn to achieve C_1=C_2:

- Increasing the size of the via or the width of the blue trace T_3 increases the capacitance C_2 and therefore reduces the asymmetry. A reduction of the red traces' area T_4 reduces the capacitance C_1.
- Changing the position of the bonds in Fig. 7 also changes the capacitances C_1 and C_2.
- The slightly colored traces T_2 and T_5 have a much smaller sensitivity and influence the front-end coupling indirectly only. The light blue colored trace T_5 beside T_4 should be increased in size to intensify the shielding of T_4 and therefore decreasing C_2 again. The opposite interpretation can be applied to the light red colored trace T_2 beneath T_3.

B. Locally Grounded Sensor

1) EEC: Similarly, Fig. 8 illustrates the minimized circuit for the locally grounded sensor in Fig. 2a. Due to a low impedance to the table, a high current flows through the locally grounded sensor. Therefore, mainly mutual inductive coupling elements contribute to the front-end coupling. The high current flows over the sensor's pin inductances (L_{GND}, L_{OUT}, L_{VDD}) and the grounding inductance (copper block) $L_{grounding}$ and couples mutually with the inductances L_1 and L_2 of the front-end.

Fig. 9 shows the LSB deviation of the PHREEC model and the minimized circuit simulation. Again, the simulations are combined with the closed-loop 300 mA BCI test setup. The minimized circuit simulations show an accuracy better 10 LSB over the whole frequency range. Only in the higher frequency range, a small deviation can be seen due to an additional capacitive coupling, which is not included in the EEC in Fig. 8.

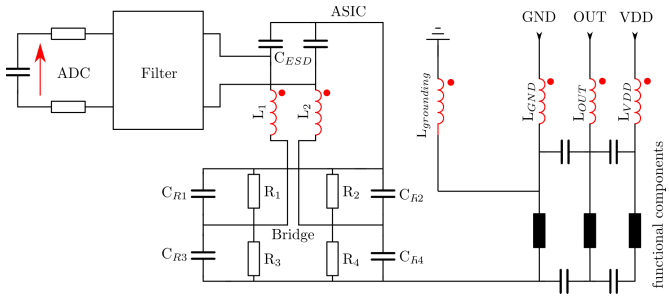

Fig. 8: EEC of a locally grounded pressure sensor when investigating the front-end coupling

Because the ADC evaluates a differential voltage, while the BCI test excites a common mode, the differential noise at the sampling capacitance arises again due to asymmetrical mutual coupling. The difference in the mutual inductances mentioned above adds up to only some pH.

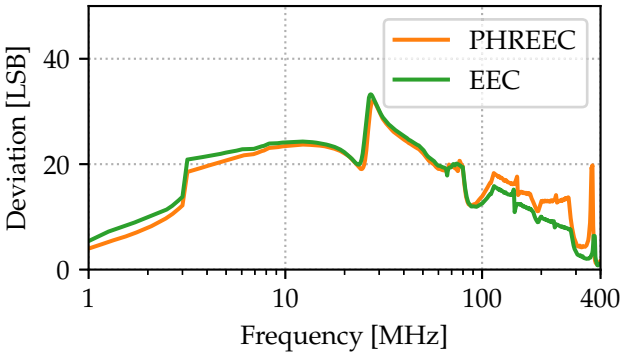

Fig. 9: Simulation of the LSB deviation using the PHREEC model and the minimized EEC model in Fig. 8 in a 300 mA closed-loop BCI test

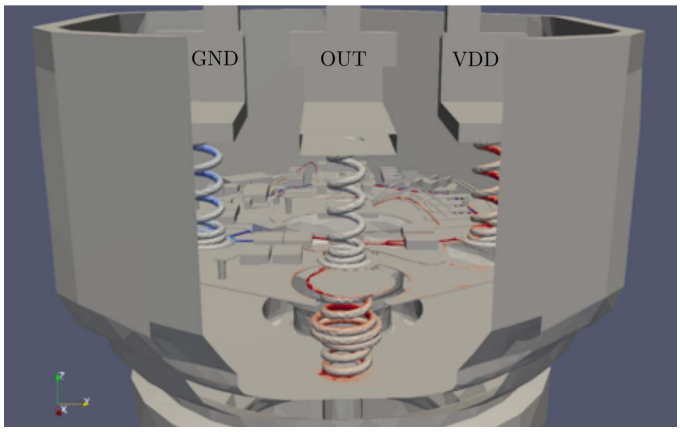

Fig. 10: 3D sensitivity analysis of the front-end coupling of the locally grounded sensor

2) 3D Sensitivity Analysis: Fig. 10 shows, in a side view, the resulting 3D sensitivity analysis of the sensor in Fig. 2a. The 3 pins (GND, OUT, VDD) are connected flexibly to the PCB via a spring. An additional spring connects the PCB ground to the housing and therefore to the common ground (table). These springs cause the largest portion of the inductances L_{GND}, L_{OUT}, L_{VDD} and $L_{grounding}$. Therefore, the springs show the biggest sensitivity and optimization potential.

3) Interpretation: The following conclusions, with the help of 3D sensitivity analysis, can be drawn:

- The lower spring connects the PCB ground to the common ground (table). Given that BCI injects mainly common mode current, most of the current flows across this spring. The red interior implies that the size should be increased to reduce the coupling. A higher impedance, due to a wider spring, causes less current to flow over the sensor and therefore decreases the coupled voltage.
- The left and right spring have opposite interior colors. Therefore, the right spring should be wider (increased inductance) while the inductance of the left spring should be decreased by making the spring smaller. This is due to the fact that the right spring is very close to the sensitive front-end bonds. Increasing the inductance of the right spring and decreasing the inductance of the left spring causes less current to flow through the right spring and therefore decreases the overall coupling.

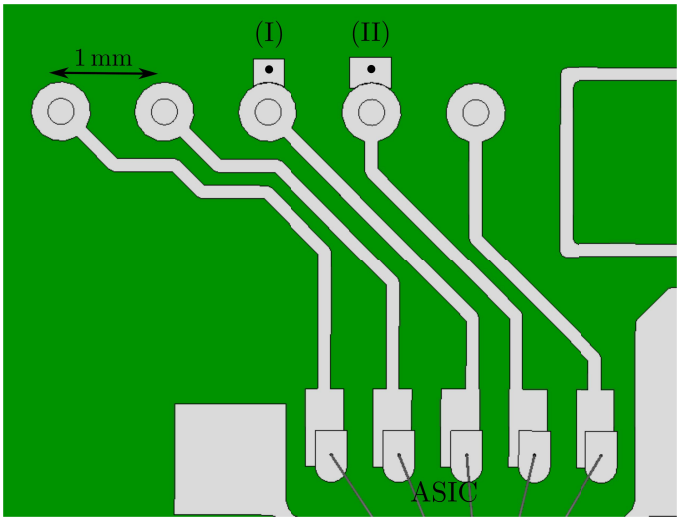

Fig. 11: Altered geometry of the front-end. (I) optimized layout (II) degraded layout

IV. Sensor Optimization

After the front-end coupling is analyzed for two different sensors and potential optimizations are derived, the following section focuses on the optimization of the sensor shown in Figs. 2b, 4, 6 and 7.

To validate the 3D sensitivity analysis, two cases with little altered geometric front-ends are simulated and measured. Therefore, little solder pads are added to the traces T_3 and T_4. The associated 3D simulations can be seen in Fig. 11. The additional pad in case (II) should degrade the immunity behavior of the sensor according to the previous interpretations of the 3D sensitivity analysis in Fig. 6. More useful and interesting is the geometric change in case (I), optimizing the sensor in a way, that it should pass the BCI test. Fig. 12 illustrates the simulation and measurement results. The measured change in the LSB deviation behaves as predicted. Adding a solder pad with a simulated capacitance to the table of around 1.5 fF in the degraded test case (II) increases the deviation by a factor of 4. Reducing the asymmetric coupling by adding a solder pad with 0.8 fF to the table to the trace T_3 improves the LSB deviation up to a factor of 4. Furthermore, the measurements are in good agreement with the equivalent circuit simulation using the EEC in Fig. 4.

V. Conclusion

The generation of physical electrical equivalent circuits in combination with a subsequent sensitivity analysis enables a

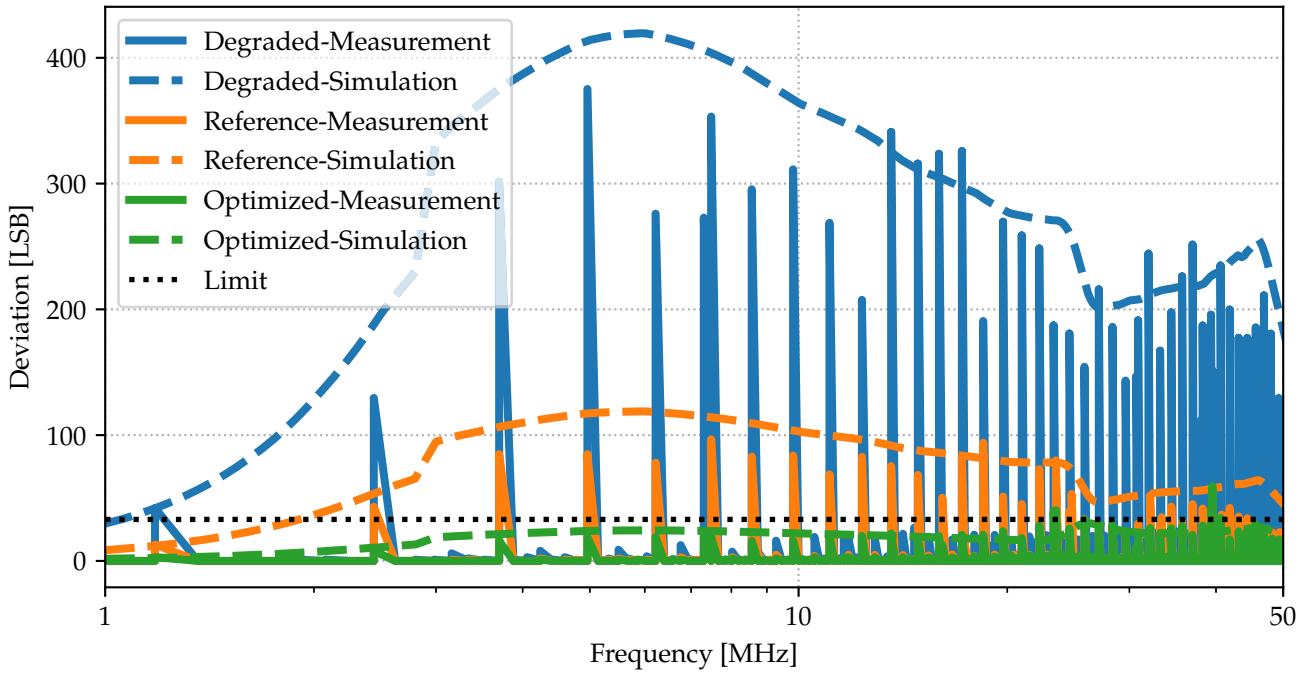

Fig. 12: 3D-simulated and measured change in the LSB deviation due to a degradation and improvement of the asymmetric, capacitive front-end coupling using a 3D sensitivity analysis

root cause analysis of small sensor devices. Furthermore, critical sensor concepts/structures can be detected before samples are available to develop design rules in advance. Additionally, 3D sensitivity analyses help with geometric optimizations in the package or layout design.

The presented methods were used to investigate the front-end coupling in automotive pressure sensors in BCI testing. With the help of sensitivity analyses, asymmetric capacitive couplings in floating sensors as well as asymmetric mutual couplings in locally grounded sensors are identified as dominant effects in reducing sensor immunity. The minimized EECs show good correlation to 3D simulations. Additional 3D sensitivity analyses led to a simple interpretation of potential layout optimizations to reduce the front-end coupling. Finally, the front-end coupling has been optimized by changing the asymmetric capacitive coupling of the investigated floating pressure sensor by less than 1 fF. A significant improvement of the EMC immunity behavior, without the need of additional filter components, is visible in measurements.

References

[1] V. Petkov, G. Balachandran, and J. Beintner, "A fully differential charge-balanced accelerometer for electronic stability control," *in IEEE Journal of Solid-State Circuits*, vol. 49, pp. 380–381, 2014.

[2] F. Fiori, "EMI-induced distortion of baseband signals in current feedback instrumentation amplifiers," *in IEEE Transactions on Electromagnetic Compatibility*, vol. 60, pp. 605–612, 2018.

[3] J. Benz, J. Hansen, and S. Frei, "Simulation and measurement of narrowband susceptibilities of digital automotive sensors," *accepted for EMC Europe*, 2019.

[4] F. Traub, J. Hansen, W. Ackermann, and T. Weiland, "Automated construction of physical equivalent circuits for inductive components," on International Symposium on Electromagnetic Compatibility, pp. 67–72, 2013.

[5] F. Traub, J. Hansen, W. Ackermann, and T. Weiland, "Generation of physical equivalent circuits using 3D simulations," on International Symposium on Electromagnetic Compatibility, pp. 486–491, 2012.

[6] F. Traub, J. Hansen, W. Ackermann, and T. Weiland, "Eigenmodes of electrical components and their relation to equivalent electrical circuits," on International Symposium on Electromagnetic Compatibility, pp. 287–293, 2013.

[7] F. Traub, "Automated construction of equivalent electrical circuit models for electromagnetic components and systems," doctoral dissertation, Technische Universität Darmstadt, 2014.

[8] S. Schuhmacher, "Sensitivitätsanalyse mittels adjungierter Verfahren für äquivalente Ersatzschaltbilder extrahiert aus 3D Feldmodellen," doctoral dissertation, Technische Universität Darmstadt, 2017.

[9] S. Schuhmacher, A. Klaedtke, and C. Keller, "Adjoint technique for sensitivity analysis of coupling factors according to geometric variations," *in IEEE Transactions on Magnetics*, vol. 54, 2018.

[10] S. Schuhmacher, A. Klaedtke, C. Keller, W. Ackermann, and H. De Gersem, "Optimizing the inductance cancellation behavior in an EMI filter design with the help of a sensitivity analysis," on International Symposium on Electromagnetic Compatibility, pp. 1–6, 2017.

[11] S. Miropolsky, A. Sapadinsky, and S. Frei, "A generalized accurate modelling method for automotive Bulk Current Injection (BCI) test setups up to 1 GHz," on 9th International Workshop on Electromagnetic Compatibility of Integrated Circuits – EMC Compo, pp. 63–68, 2013.

[12] M. Gonser, "EMV-Systemsimulation mit realen Kabelbäumen von Mess- und Prüfverfahren für Kfz-Komponenten," doctoral dissertation, Universität Erlangen-Nürnberg 2011.

[13] Y. Kondo, M. Izumichi, and O. Wada, "Simulation of Bulk Current Injection test using integrated circuit immunity macro model and electromagnetic analysis," on International Symposium on Electromagnetic Compatibility, pp. 118–122, 2016.